Lattice-Spin Mechanism in Colossal Magnetoresistive Manganites

J. A. Vergés,[1] V. Martín-Mayor,[2] and L. Brey[1]

[1]*Instituto de Ciencia de Materiales (CSIC), Cantoblanco, 28049 Madrid, Spain*

[2]*INFN, SMC-INFM, Dipartimento di Fisica, Università di Roma "La Sapienza," Piazzale A. Moro 2, 00185 Roma, Italy*

(Received 6 September 2001; published 14 March 2002)

We present a single-orbital double-exchange model, coupled with *cooperative* phonons (the so called breathing modes of the oxygen octahedra in manganites). The model is studied with Monte Carlo simulations. For a finite range of doping and coupling constants, a first-order metal-insulator phase transition is found, which coincides with the paramagnetic-ferromagnetic phase transition. The insulating state is due to the self-trapping of every carrier within an oxygen octahedron distortion.

DOI: 10.1103/PhysRevLett.88.136401 PACS numbers: 71.38.–k, 75.10.–b

Mixed-valence manganites have attracted much attention lately, since they undergo a transition from a ferromagnetic (F) to a paramagnetic (P) state accompanied by a metal (M) to insulator (I) transition. The double exchange (DE) mechanism [1] plays a major role in explaining the magnetic transition, but the mechanism responsible of the *M-I* transition is not fully understood [2]. In the DE model, due to a very strong Hund's coupling, the carriers are strongly ferromagnetically coupled to the Mn core spins producing a modulation of the hopping amplitude between Mn ions. Recently a growing number of experiments [3–6] have supported the idea that phase separation is important in manganites [7–9]. In this state, a phase is metallic and the other insulating. The theoretical challenge is thus to find a *FM-PI* phase transition of the first order. Whereas it is widely assumed that the metallic phase is the ferromagnetic DE phase, it is not clear what is the origin of the gap in the insulating phase. For doping level near half filling and low critical temperature (T) materials, it has been proposed and widely accepted that the insulator is a charge-orbital ordered phase with a strong short range order. At lower doping levels the insulating phase is supposed to be some kind of polaron gas [10,11] (polaron meaning a lattice-spin object) or polaron lattice phase [12,13].

An attractive picture for polaron formation was presented in Refs. [10,11]: it was observed that the importance of the electron-lattice coupling is given by its ratio with the carriers kinetic energy. Since within the DE mechanism the kinetic energy decreases upon heating, it was proposed that localized polarons are formed at the *F-P* transition giving rise to a *M-I* transition. Millis *et al.* [10] used the dynamical mean-field method to study the coupling of the carriers to local Jahn-Teller distortions and to the Mn core spins. At half filling an *I-M* transition was found close to the Curie T. It was shown that the electron-phonon coupling could be tuned to reproduce the T dependence of the resistivity of several manganites. Unfortunately, this approach presented several caveats: the *M-I* transition was found only at half filling, phonons are treated classically, and (most important) intersite phonon correlations were not considered.

In this Letter, we consider a single-orbital (s-wave) DE model coupled with phonons. The model will be kept as simple as possible, since our scope is to shed some light on the mechanism behind the coupling between the *M-I* transition and the Curie temperature. Both core spins and phonons are treated as classical variables (for spins this is a controlled approximation [14]). The lattice distortion we study is the deformation of the oxygen octahedra around Mn sites. The coupling of these modes with charge carriers is expected to be at least as large as the one producing Jahn-Teller distortions [15]. The contraction (*breathing*) of a MnO_6 octahedron, implies a volume growth of its neighbors (but does not change the total lattice volume, as would be needed to study magnetostriction effects [16]). Thus this mode is strongly cooperative, and not suitable for mean-field studies. A Monte Carlo (MC) investigation is therefore performed. The superexchange antiferromagnetic coupling between the core spins [17] is neglected in our model. Also, as we mentioned above, we work with a single s orbital per site and we do not consider the two degenerated $\mathbf{e_g}$ orbitals which are crucial to understanding the magnetic phase-diagram beyond half filling [18]. Thus, our model is to be regarded as a model for materials such as $La_{1-x}Ca_xMnO_3$ in the $0.15 < x < 0.4$ regime where the magnetoresistance is largest, and the only experimentally relevant magnetic phases are F and P [2]. In spite of its simplicity, the model presents a first-order *M-I* phase transition, that coincides with the *P-F* phase transition *for a finite range of doping* and coupling constants, in contrast with previous work [10].

The model Hamiltonian contains the Mn $\mathbf{e_g}$ itinerant carriers coupled to the $\mathbf{t_g}$ Mn core spins, and phonons:

$$H = H_{\mathrm{KE}} + H_{\mathrm{Hund}} + H_{\text{el-ph}} + H_{\mathrm{ph}} . \qquad (1)$$

Here H_{KE} is the kinetic energy of the carriers hopping between Mn atoms that form a simple-cubic lattice, H_{Hund} is the Hund interaction, $H_{\text{el-ph}}$ is the lattice-carrier coupling energy, while H_{ph} represents the crystal elastic energy. The Hund interaction is very large in manganese oxides and at each place the carrier spin is forced to be parallel to the core spin, which allows us to reduce $H_{\mathrm{KE}} + H_{\mathrm{Hund}}$ to the DE Hamiltonian [8]:

$$H_{\mathrm{DE}} = \sum_{\langle i,j \rangle} [\mathcal{T}(\boldsymbol{S}_i, \boldsymbol{S}_j) c_i^{\dagger} c_j + \mathrm{H.c.}]. \quad (2)$$

Here c_i^+ creates an electron at place i with spin parallel to the core spin at i, t is the hopping amplitude between first neighbors ions and $\mathcal{T}(\boldsymbol{S}_i, \boldsymbol{S}_j) = -t[\cos\frac{\theta_i}{2}\cos\frac{\theta_j}{2} + \sin\frac{\theta_i}{2}\sin\frac{\theta_j}{2}e^{i(\varphi_i - \varphi_j)}]$, θ_i and ϕ_i being the polar coordinates of the core spin at site i, $\boldsymbol{S}_i$. For the electron-phonon coupling we consider the distortions of the MnO_6 octahedron formed by the six oxygens surrounding the Mn ions. The oxygens are located at the center of the edges of the cubic lattice formed by Mn atoms. Each oxygen is allowed to move along the edge on which it is located. The distortions of the six oxygens surrounding a Mn at site i are given by $u_{i,\pm\alpha}$ where α run over x, y, z. The size fluctuations of the MnO_6 octahedra are coupled to charge fluctuations in the Mn through the electron-phonon interaction,

$$H_{\text{e-ph}} = -\lambda t \sum_{i,\alpha} (u_{i,-\alpha} - u_{i,\alpha}) c_i^{+} c_i \,, \quad (3)$$

where λ is the electron-phonon coupling. This interaction tends to produce lattice distortions. This tendency is opposed by the stiffness of the Mn-O bonds:

$$H_{\mathrm{ph}} = t \sum_{i,\alpha} (u_{i,\alpha})^2. \quad (4)$$

One can get some intuition about the physics of our model considering the limit of very few carriers. If the carrier-lattice coupling is strong, one can gain enough electronic energy by contracting an oxygen octahedron (thus localizing a carrier: a *polaron*) to compensate the high price in elastic energy. For the fully spin-polarized lattice, one finds (using, e.g., the techniques of Ref. [19]) $\lambda^{\text{threshold}} = 1.91$. The carrier is localized at the polaron's center with a 96% probability. If one repeats the calculation for the P phase, using deGennes' virtual-crystal approximation [20], finds $\lambda^{\text{threshold}} \approx 1.56$ (the P polaron is also at its center with 96% probability). Thus for λ in between both thresholds, one expects that at the F-P phase transition, every carrier will form a strongly localized polaron upon heating. The system becomes insulating due to the formation of a fully occupied band separated from upper states by a gap. This picture is largely confirmed by the MC simulation of the model.

For calculating the T-dependent phase diagrams, we perform MC simulations on the classical variables: the core spins $\boldsymbol{S}_i$ and the oxygen displacements $(u_{i,\alpha})$. The simulations are done in $N \times N \times N$ lattices with periodic boundary conditions, using a standard Metropolis algorithm. The kinetic energy of the carriers is calculated by diagonalizing the electron Hamiltonian at each Metropolis step. The diagonalization CPU cost grows like N^6 and has limited us to $N = 6$ [21]. We have used the $N = 4$ results to check for finite-size effects. Although both absolute values and details sometimes change for $N = 4$ simulations, all issues discussed in this Letter remain valid. The Fermi temperature of the carriers is much higher than other T in the system and we assume the carriers to be at zero T [23]. We calculate the thermal average of different physical quantities; the absolute value of the $\boldsymbol{S}_i$ polarization, M, the electronic energy difference between the lowest energy empty state and the highest energy occupied one, E_{gap}, the standard deviation of the (spatial) probability distribution of the MnO_6 octahedra volume, ΔV_{rms}, and the electronic density of states, $\rho(\omega)$. We also measure the average dc resistance of the system, calculating the resistance of the $N \times N \times N$ cubic lattice connected to two semi-infinite perfect leads [24,25] using the standard Kubo formula [26].

Figure 1 shows the phase diagram, λ vs T, for a $N = 6$ cubic lattice with 17 electrons, i.e., $x \simeq 0.08$. We use the criterion that the system is M/I when the dc resistance increases/decreases with T. The phase diagram contains four phases: FM, FI, PM, and PI. As expected for small λ, polarons are not formed by the (small) lattice distortions, the system being metallic at all T [23,25] (see the growing behavior of the dc resistance upon heating in Fig. 2—bottom). When T grows there is a second order FM-PM transition (see the smooth temperature behavior of M in the top of Fig. 2). At $\lambda = 0$, we found the Curie T at $0.072t$, in agreement with previous MC simulations at $x = 0.08$ [23]. Notice that thermodynamic quantities are even functions of λ [because of the symmetry $\lambda \to -\lambda$, $u_{i,\alpha} \to -u_{i,\alpha}$ in Eq. (1)], and thus for small couplings they quadratically depend on λ. This can be checked for the Curie T in Fig. 1.

At intermediate λ, new behavior is expected. In the P phase (that has higher energy than the F phase), all carriers form polarons and the system is an insulator, while in the F phase there are not polarons and the system is metallic. Upon heating, the degenerated electronic system undergoes a phase transition at the F-P transition, with a sharp change in electronic energy. A first-order F-P

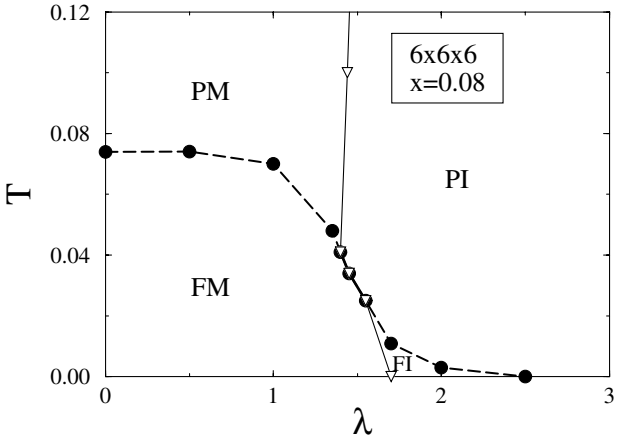

FIG. 1. The T (in units of t)-λ phase diagram of the model (1), obtained from MC simulations on a 6^3 lattice with $x = 0.08$ (see text). Filled dots: P-F critical T. Open triangles: M-I critical T.

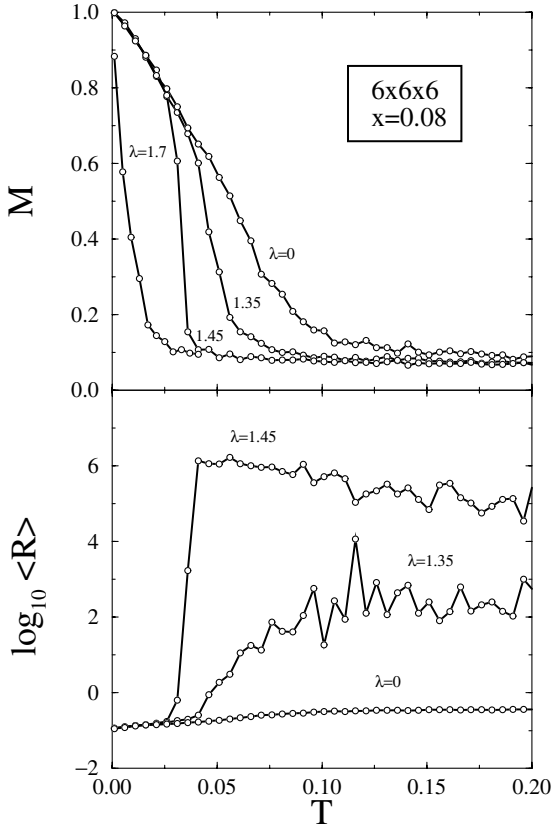

FIG. 2. Top: M vs T for $\lambda = 0, 1.35, 1.45$, and 1.7, for the MC simulations in Fig. 1. Bottom: (decimal) logarithm of the average dc resistance (a.u.) vs T, from the same simulations ($\lambda = 1.7$ data are out of range).

phase transition with growing T is obtained, that coincides with a *M-I* transition. Indeed, Fig. 1 shows how the *P-M* and *I-M* transition lines merge for $1.4 < \lambda < 1.65$. M changes abruptly at the phase transition (Fig. 2, top) while the dc resistance grows by a factor 10^6 (Fig. 2, bottom) and becomes a decreasing function of T. First-order *P-F* transitions are experimentally found in manganites as the strength of the electron-phonon coupling increases [27]. For slightly smaller values of λ ($\lambda = 1.35 < \lambda_c = 1.4$) the dc resistance always grows with T, the system being M, and the *F-P* phase transition is continuous (Fig. 2, top and bottom). Polaron formation can also be seen in the spatial distribution of volumes of the MnO_6 octahedra that becomes very inhomogeneous: on polarons, octahedra are small while in most sites the volume is uniform. Note the sharp change of $\Delta V_{\rm rms}$ at the critical line for $1.4 < \lambda < 1.7$ (Fig. 3), and the smoother T dependence for $\lambda = 1.35$. Notice also (Fig. 4) the gap in $\rho(\omega)$ for $1.4 < \lambda < 1.7$ (the Fermi level is in the gap).

For large λ, polarons exist in both the P and F phases. The *F-P* and the *M-I* transitions decouple for $\lambda > 1.65$ (Fig. 1). The *F-P* one is again continuous: M evolves smoothly with T (Fig. 2, top), and the system has polarons at the lowest T (Fig. 3), being an *I*. The *F* phase in a DE

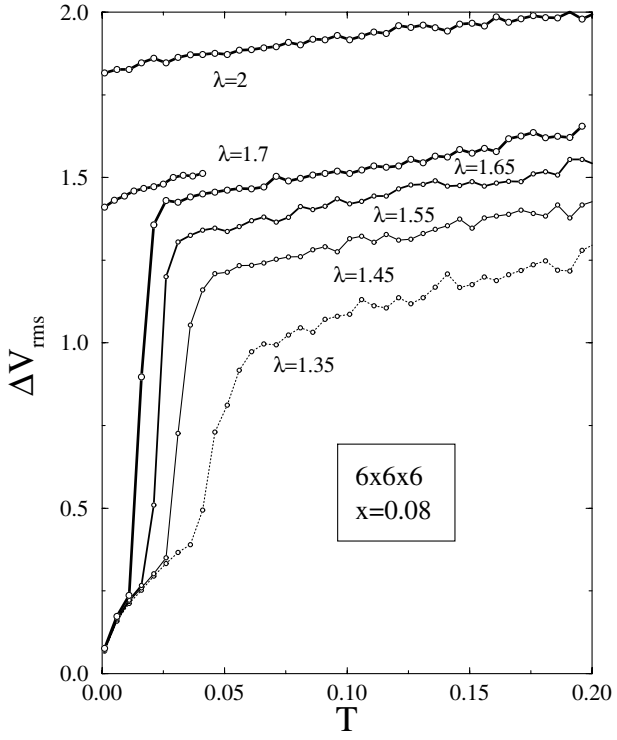

FIG. 3. Standard deviation of the (lattice) distribution of the volume of the MnO_6 octahedra vs T, for the simulations in Fig. 1.

system with a fully occupied band is somehow unconventional, because the mean carriers energy is at the band center which is usually spin independent. This is not the case for our model. The difference between the positions of the (polaronic) band center of the fully polarized and unpolarized systems can be calculated as before, with de Gennes' virtual-crystal approximation. The energy difference for large λ is roughly $-1.08t/\lambda^2$ which explains the (small) ferromagnetic interaction that decreases with increasing λ.

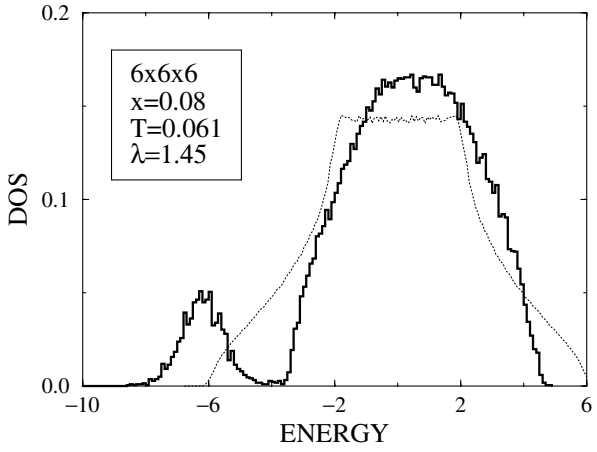

FIG. 4. Thermal average of the electronic density of states for $\lambda = 1.45$, $T = 0.061$ (*PI* phase in Fig. 1). The dashed line is the density of states of the fully spin-polarized system, without octahedra distortions.

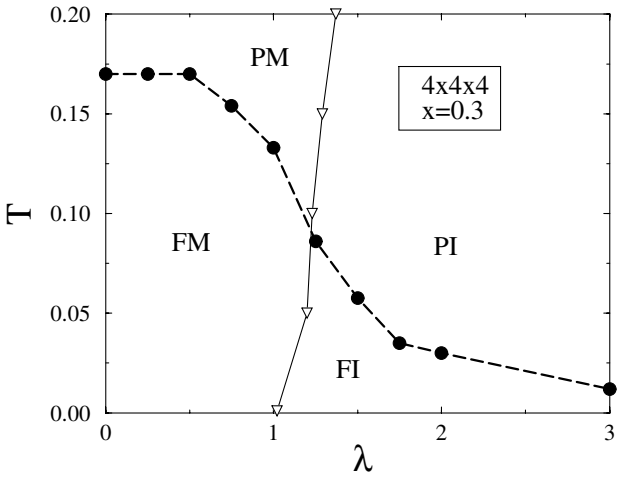

FIG. 5. Phase diagram for the model (1), as obtained from the MC simulation on 4^3 lattices at $x = 0.29$. Filled dots: the *F-P* critical T. Open triangles: *M-I* critical T.

The results shown up to now can be understood qualitatively and semiquantitatively within the few carriers limit. However, when the polaron density approaches the percolation threshold of the cubic lattice ($p_c = 0.31$ [28]), the polaronic wave function becomes far less localized. In Fig. 5, we show the phase diagram for $x = 0.3$. We find the same phases as in the $x = 0.08$ case. In the *I* case, all carriers are polarons. Notice the absence of a coupling between the *P-M* and the *M-I* transitions, the former being of the second order. Therefore in our model, we do not get a T-dependent *M-I* transition at $x = 0.3$. Nevertheless, our model only includes an orbital per Mn ion. The use of a more realistic band structure will increase the phase space for the polarons and a T-dependent *M-I* transition will occur also at higher doping levels.

In summary, we have studied a DE model coupled with the breathing modes of the MnO_6 octahedra. Given the collective nature of these modes, the spatial distribution of the lattice distortions is inhomogeneous and a mean-field study difficult. A thorough MC investigation of the phase diagram has been carried out. Four phases have been found: *FM*, *FI*, *PM*, and *PI*. A first order *M-I* transition with growing T (coincident with the *F-M* transition) has been found for the first time on a MC simulation. This transition survives for a finite range of doping and coupling constant. The *M-I* transition is induced by the self-trapping of every carrier on a polaron, making the Fermi level to lie on the gap between the polaronic and DE bands (for $t \approx 0.16$ eV [2], the gap will be optical). We argue that the mechanism presented here is relevant for the formation of the paramagnetic-insulating phase experimentally observed in the phase-separated state of colossal magnetoresistive manganites [3–6].

We are grateful to F. Guinea, J. L. Alonso, and S. Fratini for discussions. Financial support is acknowledged from Grants No. PB96-0085 (MEC, Spain) and CAM-07N/0008/2001 (Madrid, Spain). V. M-M. is partially supported by E.C. Contract No. HPMF-CT-2000-00450.

[1] C. Zener, Phys. Rev. **82**, 403 (1951); P. W. Anderson and H. Hasegawa, *ibid.* **100**, 675 (1955); P. G. deGennes, *ibid.* **118**, 141 (1960).
[2] See, for example, A. P. Ramirez, J. Phys. Condens. Matter **9**, 8171 (1997); J. M. D. Coey, M. Viret, and S. von Molnar, Adv. Phys. **48**, 167 (1999); Y. Tokura, J. Magn. Magn. Mater. **200**, 1 (1999).
[3] M. Jaime *et al.,* Phys. Rev. B **60**, 1028 (1999).
[4] R. H. Heffner *et al.,* Phys. Rev. Lett. **85**, 3285 (2000).
[5] C. P. Adams *et al.,* Phys. Rev. Lett. **85**, 3954 (2000).
[6] T. Wu *et al.,* Phys. Rev. Lett. **86**, 5998 (2001).
[7] D. Arovas, G. Gómez-Santos, and F. Guinea, Phys. Rev. B **59**, 13 569 (1999).
[8] See the review by E. Dagotto *et al.,* Phys. Rep. **344**, 1 (2001).
[9] J. Burgy *et al.,* Phys. Rev. Lett. **87**, 277 202 (2001).
[10] A. J. Millis *et al.,* Phys. Rev. Lett. **77**, 175 (1996); Phys. Rev. B **54**, 5405 (1996).
[11] H. Roder *et al.,* Phys. Rev. Lett. **76**, 1356 (1996).
[12] N. D. Mathur and P. B. Littlewood, cond-mat/0104238.
[13] T. Mizokawa *et al.,* cond-mat/0011070.
[14] D. P. Arovas and F. Guinea, Phys. Rev. B **58**, 9150 (1998); M. Yu. Kagan, D. I. Khomskii, and M. V. Mostovoy, Eur. J. Phys. B **12**, 217 (1999).
[15] A. J. Millis, Phys. Rev. B **53**, 8434 (1996).
[16] J. M. de Teresa *et al.,* Nature (London) **386**, 256 (1997).
[17] The inclusion of antiferromagnetic coupling between core spins can lead to more sophisticated magnetic phase diagrams. See, for example, J. L. Alonso *et al.,* Phys. Rev. B **64**, 54 408 (2001); **63**, 64 416 (2001); **63**, 54 411 (2001); D. P. Arovas and F. Guinea, Phys. Rev. B **58**, 9150 (1998).
[18] J. van den Brink *et al.,* Phys. Rev. Lett. **83**, 5118 (1999); T. Mizokawa *et al.,* Phys. Rev. B **61**, R3776 (2000).
[19] V. Martín-Mayor *et al.,* Phys. Rev. E **62**, 2373 (2000).
[20] See de Gennes in Ref. [1].
[21] In the case of gapless systems, more powerful techniques are available [22], but for systems with a gap they have not been tested yet.
[22] J. L. Alonso *et al.,* Nucl. Phys. **B569**, 587 (2001).
[23] M. J. Calderón and L. Brey, Phys. Rev. B **58**, 3286 (1998).
[24] J. A. Vergés, Phys. Rev. B **57**, 870 (1998).
[25] M. J. Calderón, J. A. Vergés, and L. Brey, Phys. Rev. B **59**, 4170 (1999).
[26] A. Bastin *et al.,* J. Phys. Chem. Solids **32**, 1811 (1971).
[27] J. Mira, J. Rivas, F. Rivadulla, C. Vázquez-Vázquez, and M. A. López-Quintela, Phys. Rev. B **60**, 2998 (1999).
[28] D. Stauffer and A. Aharony, *An Introduction to Percolation Theory* (Taylor & Francis, London, 1994).